Bridging the Gap: *OPTICAM* Reveals the Hidden Spin of the WZ Sge Star *GOTO 065054.49+593624.51*

N. Castro Segura[©] 1,2*, Z. A. Irving[©] 2, F. M. Vincentelli[©] 2, D. Altamirano[©] 2, Y. Tampo[©] 3,4, C. Knigge[©] 2, I. Pelisoli[©] 1, D. L. Coppejans[©] 1 N. Rawat³, A. Castro[©] 5,2, A. Sahu[©] 1, J. V. Hernández Santisteban[©] 6, M. Kimura⁸, M. Veresvarska[©] 7, R. Michel[©] 5, S. Scaringi[©] 7,10 & M. R. Najera[©] 5.

Affiliations are listed at the end of the paper

Accepted XXX. Received YYY; in original form ZZZ

ABSTRACT

WZ Sge stars are highly evolved accreting white dwarf systems (AWDs) exhibiting remarkably large amplitude outbursts (a.k.a. super-outbursts), typically followed by short rebrightenings/echo outbursts. These systems have some of the lowest mass transfer rates among AWDs, making even low magnetic fields dynamically important. Such magnetic fields are often invoked to explain the phenomenology observed in these systems, such as their X-ray luminosity and long periods of quiescence (30+ years). However, the detection of these is very elusive given the quenching of the accretion columns during outburst and the low luminosity of these systems during quiescence. Here we present high-cadence multi-band observations with *OPTICAM* of the recent outburst of the recently discovered WZ Sge star GOTO065054.49+593624.51, during the end of the main outburst and the dip in-between rebrightenings, covering 2 orders of magnitude in brightness. Our observations reveal the presence of a statistically significant signal with $P_{\omega} \approx 148$ seconds in the bluer (g) band which is detected only during the dip between the main outburst and the rebrightenings. We interpret this signal as the spin period of the AWD. If confirmed, GOTO 0650 would bridge the gap between intermediate- and fast-rotating intermediate polars (IPs) below the period gap.

Key words: accretion, accretion discs – stars: dwarf novae – stars: individual: GOTO065054.49+593624.51

1 INTRODUCTION

Cataclysmic variable stars (CVs) are binary systems in which a lowmass secondary star, filling its Roche lobe, transfers mass to a white dwarf (WD) primary. In systems where the magnetic field is dynamically unimportant, the accretion process is mediated by an accretion disc. If the magnetic field of the WD is sufficient to prevent the formation of the disc, this gives rise to the so-called *polars*. If, on the other hand, a disc can form but is truncated by the magnetosphere of the central WD, the systems are traditionally classified as intermediate-polars (IPs), however, recent findings suggest that some IPs may be disc-less (e.g. Littlefield et al. 2021). Disc-mediated systems with mass transfer rates sufficiently low to prevent the disc from remaining persistently in a fully ionized state are classified as Dwarf novae (DNe; see e.g. Warner 1995, for a review on CVs). DNe are characterized by exhibiting eruptions where the system brightens typically 2-5 magnitudes for a relatively short period of time. Such eruptions are thought to be the consequence of a sudden increase in the mass accretion rate onto the compact object due to the accretion disc transitioning from a neutral to a fully ionized state (e.g., Lasota 2016).

WZ Sge-systems are highly-evolved short orbital period DNe which exhibit even larger amplitude outbursts (up to $\sim 8-9$ mag). These so-called super-outbursts are characterized by prolonged out-

* E-mail: N.Castro-Segura@warwick.ac.uk

burst durations (approximately 30 days), and the appearance of superhumps — low-amplitude variations near the system's orbital period — shortly after reaching peak brightness (Smak 1993, 2009; Patterson et al. 2005; Kato 2015; Hameury 2020). These super-outbursts are typically followed by a series of short-term rebrightenings or echo outbursts which seem to be characteristic of accreting binaries with extreme mass-ratios. These rebrightenings cannot be explained by the standard disc instability model (DIM; e.g. Hameury 2020). To reconcile observations with theoretical predictions, Campana et al. (2018) recently proposed an alternative explanation where the luminosity drops during outburst decay signal a temporary transition to a magnetic propeller state. This is an appealing framework as it could help to explain the behaviour of accreting systems at different scales, i.e. X-ray binaries, young stellar objects and CVs. This framework also aligns well with the proposed spin period of 27.87 seconds of WZ Sge (Patterson 1980; Patterson et al. 1998). However, using HST time-resolved spectroscopy, Georganti et al. (2022) showed that WZ Sge does not exhibit any propeller footprint during the proposed propeller state (c.f. Eracleous & Horne 1996). Nonetheless, truncation of the inner disc is required to explain the relatively high X-ray luminosity. Against this background, Hameury (2020) proposed that the X-ray excess observed in WZ Sge could (also) be a consequence of evaporation of the inner disc, while the quiescent phases between outbursts are produced by overflows of the mass-transfer stream impacting the inner regions of the disc, similar to what is proposed to explain IW And-systems and some nova-like CVs (Kimura et al.

2020; Castro Segura et al. 2021). Regardless of whether magnetic fields are responsible for the X-ray luminosities in WZ Sge stars, they are often invoked to explain the very long recurrence timescales in these systems (Kato 2015).

In this Letter we report high cadence multi-band photometry of the newly discovered transient GOTO065054.49+593624.51 (hereafter GOTO 0650) obtained with OPTICAM (Castro et al. 2019, 2024). GOTO 0650 was discovered by the Gravitational-wave Optical Transient Observer (GOTO; Steeghs et al. 2022; Dyer et al. 2024) on Oct. 4 2024 03:36:36 UT (Killestein et al. 2024a). The transient reached an L band ($\sim g + r$) magnitude of 13.7 in the discovery images and was associated with a $\sim 22^{nd}$ mag quiescent counterpart implying an outburst amplitude of ~ 8.5 mag, typical of WZ Sge stars. The nature of the transient was confirmed by spectroscopic observations and ultraviolet photometry (e.g. Killestein et al. 2024b; Bhattacharya & Bhattacharyya 2024). Using data from the American Association of Variable Star Observers (AAVSO) and the Zwicky Transient Facility (ZTF; Bellm et al. 2019a,b), we show in Figure 1 how the outburst evolution and rebrigthenings are consistent with the classification above. Tampo (2024) reported the onset of regular super-humps after a type-E recovery of a dip ~ 15 d from the beginning of the outburst (e.g. Kimura et al. 2018), and suggested GOTO 0650 is a period bouncer with an orbital period close to the superhump period ($P_{sh} = 91.05 \pm 3 \text{ min}$), again, in line with GOTO 0650 being a member of the WZ Sge-type DNe.

2 OBSERVATIONS AND DATA REDUCTION

The OPtical TIming CAMera (OPTICAM; Castro et al. 2019, 2024) is a new high-cadence, multi-band camera mounted on the 2.1-meter telescope at the San Pedro Mártir Observatory (OAN-SPM), in México. OPTICAM is equipped with three Andor Zyla 4.2-Plus sCMOS cameras with three 2048 × 2048 pixels and a set of SDSS filters (ugriz), allowing coverage in the $3200AA - 1.1\mu m$ range. The field of view (FoV), is $\approx 5 \times 5$ arcmin² with a pixel-scale of $\approx 0.15''/\text{pix}$. GOTO 0650 was observed in the g, r, i bands during the nights of October 26, 28, 30 and November 2^{nd} and 4^{th} of 2024. The sky conditions were photometric for all the nights except for the last one, during which variable high clouds were present; this is reflected in our ability to recover the i band photometry in epoch 5. The details of the observations can be found in Table 1. The data were primarily reduced using version 1.13.0 of the photutils Python package (Bradley et al. 2024). Cosmic rays were clipped from all images using the L.A.Cosmic algorithm (van Dokkum 2001) as implemented in Astro-SCRAPPY version 1.2.0 (McCully et al. 2018). For each image, two dimensional background images were calculated using the SExtractorBackground estimator from photutils with a box_size of 64 pixels for 2×2 binning or 42 pixels for 3×3 binning. Image segmentation was used to identify sources in the background and subtracted images using the SourceFinder routine from photutils, which combines source detection and deblending. To identify sources, we set the npixels parameter to 32 pixels for 2×2 binning and 14 pixels for 3×3 binning. The threshold parameter was set to 5×background RMS, and the background RMS was estimated using StdBackgroundRMS. All other parameters were left to their default values.

We used the optimal photometry algorithm described in Naylor (1998) to perform photometry on the background-subtracted images. We model the PSF of *OPTICAM*'s three cameras using two-dimensional Gaussians for each camera. We stacked the images from each epoch for each camera to get the PSF parameters. We then iden-

Table 1. Observing log. The star in the epoch number denotes statistically significant detection of short-term periodicity (see Sec. 3 for details).

Epoch	MJD _{start}	filters	exposure time	obs. length	binning
	day		seconds	hours	
1	60609.31	gri	3	4.65	2 × 2
2	60611.33	gri	3	4.54	2×2
3	60613.38	gri	5	3.62	2×2
4*	60616.39	gri	15	3.34	3×3
5	60618.29	gri	15	5.89	3×3

tified sources in the stacked images using SourceFinder, which assigns a semi-major and semi-minor standard deviation to each source. The PSF for each camera in each epoch was then modelled using the median semi-major and semi-minor standard deviations from the corresponding stacked image. We then used differential photometry to correct for atmospheric variability; relative light curves were computed using the summed fluxes of the same (non-variable) reference stars in each night.

3 ANALYSIS AND RESULTS

The high cadence photometric light curves are presented in the left panels of Figures 2 and 3, the comparison stars in these figures are always the same (namely Gaia EDR3 1003219393009879424 and 1003225264228638336), so the change in relative flux between epochs is meaningful. As can be seen in Figure 1, epochs 1 and 2 were taken towards the end of the superoutburst, epoch 3 was taken during the decline, epochs 4 and 5 occurred during the dip between the main outburst structure and the rebrightenings, when the source was $\sim 4-5$ mags fainter than the first observation but ~ 3 mags brighter than the quiescent level. During epochs 1-3, the source was dominated by the regular superhumps reported by Tampo (2024), with the dispersion in the light curves reducing as the accretion disc got fainter. In epochs 4 and 5 there is still a slow modulation present with similar frequency as before, as can be seen in Figure 3, the general trend is similar but the g-band exhibits higher amplitude (than at least the r-band). In both of these epochs, we can see short-term variability in the g-band, suggesting the presence of an additional component contributing to the modulation of the light curve.

To characterise the short term variability of *GOTO 0650* we have computed the generalized Lomb-Scargle periodogram (LSP; Lomb 1976; Scargle 1982; VanderPlas 2018a) for each light curve as implemented in astropy version 6.1.2. We normalised our LSPs according to:

$$P = 2\delta t P_{\rm LSP},\tag{1}$$

where δt is the time resolution of the light curve and $P_{\rm LSP}$ represents the *unnormalised* LSP powers. This normalisation is defined such that the integrated periodogram yields the variance of the light curve (Vaughan et al. 2003).

To estimate the confidence levels of the proposed signals in our LSPs, we model the continuum analytically following the method described in Appendix A of Vaughan (2005), which we note is only applicable to the LSP if the time series is uniformly sampled and the LSP is evaluated at the Fourier frequencies (VanderPlas 2018b).

Provided the time series is uniformly sampled and the LSP is evaluated at the Fourier frequencies.

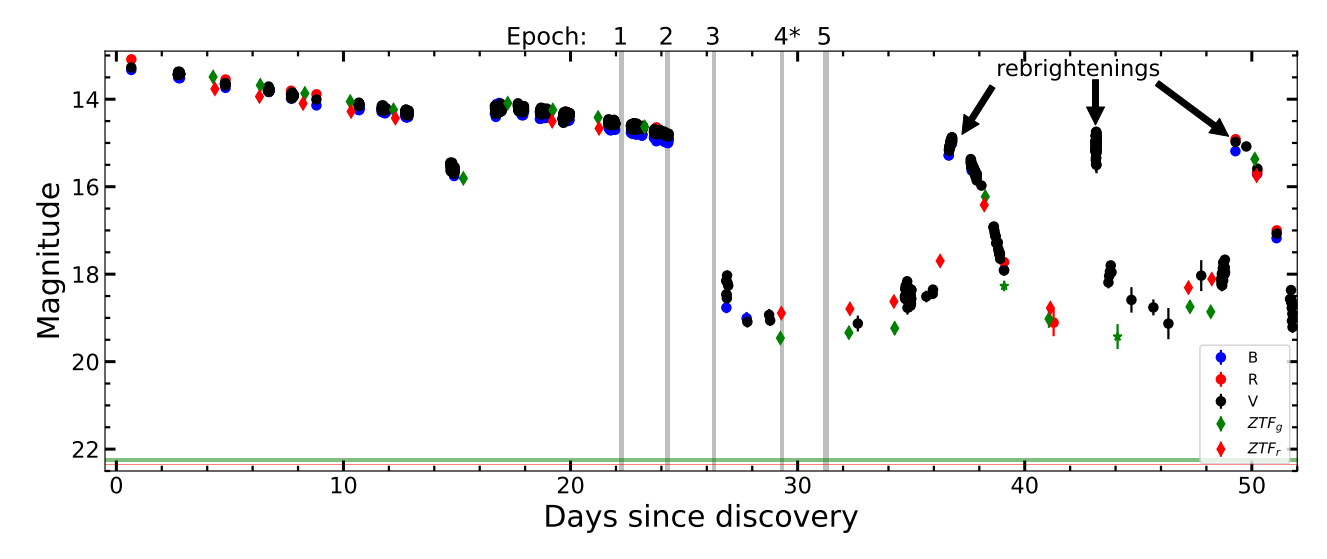


Figure 1. Outburst evolution of *GOTO 0650* as reported by the AAVSO (circles) and ZTF (diamonds for psf- and stars for forced-photometry). The different colours indicate the magnitude in different bands. The coloured horizontal bands encompass the $\pm 1\sigma$ error around the weighted mean of the quiescent photometry obtained with forced photometry on ZTF during 9-25 days before the onset of the superoutburst, the precise values are $g = 22.25 \pm 0.03$ mag and $r = 22.351 \pm 0.005$ mag. The arrows highlight the maxima of the post-outburst re-brightening/-flares. The time of the high-cadence observations with *OPTICAM* are indicated with the grey shaded regions, the epoch ID for each observation reported in this paper is indicated on the top axis. (*) denotes the epoch with a statistically significant detection of the 148s signal.

We compute confidence thresholds by scaling our continuum model by $-2\ln(\epsilon/n')$, where ϵ is the desired false alarm probability and n' is the number of LSP ordinates used to fit the model. The LSP for each of the light curves is shown in the right panel of Figures 2 and 3. We found a periodicity of $P_{\omega} = 148.2$ s with more than 99.99 per cent confidence only in the g-band of epoch 4, though we also note a non-statistically significant signal at the same frequency in the r band of the same epoch (72.25 per cent confidence). In turn, we are not able to recover any signal from the LSP but, despite this, the g-band lightcurve from that same epoch exhibits short-term flares qualitatively similar to those observed in epoch 4. We derive the analytical false alarm probability of our epoch 4 g-band detection to be 1.16×10^{-6} ; the probability of detecting a signal of this significance in at least one of our 14 LSPs by chance (i.e., when there is no underlying signal) is 0.0016 per cent.

To determine the centre and 1σ uncertainty of the frequency detected in epoch 4, and the coherence of this modulation, we performed a bootstrap analysis (e.g. Ivezić et al. 2014). We note that bootstrapping can also be used to reject sampling aliases (e.g., Southworth et al. 2006), which may be present in the *i*-band LSP. From this analysis, we found peak frequencies of 6.73 ± 0.02 mHz (*g*-band), 6.73 ± 0.02 mHz (*r*-band), and 6.75 ± 0.02 mHz (i-band). These frequencies correspond to periods of 148.5 ± 0.4 s, 148.7 ± 0.4 s, and 148.2 ± 0.5 s, respectively. To further test the coherence, we fit a Lorentzian to the Epoch 4 *g*-band periodogram (Belloni et al. 2002) on top of our noise model (Vaughan 2005, top right panel in Figure 3) and found a Q factor of 3422. The bootstrapped uncertainties and high Q factor are both indicative of a highly coherent signal.

To visualise the modulations identified in Epoch 4, we phase folded these light curves on the peak frequencies inferred via our bootstrap analysis; we present these phase folded light curves in Figure 4, along with localised LSPs. Prominent modulations are only apparent in the g-band, with a peak-to-peak amplitude of roughly 10 per cent (compared to an average 1σ white noise amplitude of 2.6 per cent). The 3σ upper limits using the average white noise amplitude for the Epochs 1, 2, 3 and 5 in g-band is 4.8, 4.5, 14.5 and 10.5 per cent re-

spectively. For the LSPs, 99.99 per cent confidence thresholds were estimated by simulating 10,000 white-noise light curves for each band. Each simulated light curve had the same time sampling as the observed light curve, and fluxes were generated from the following Gaussian $f_i \sim \mathcal{N}(\bar{f}, \sigma_{f_i})$, where \bar{f} represents the mean flux of the observed light curve and σ_{f_i} represents the uncertainties on the observed flux values. As can be seen in Figure 3, the periodograms of Epoch 4 are white-noise-dominated beyond 5 mHz, and so our estimated confidence thresholds are unlikely to be significantly biased in this frequency range.

To test the veracity of the signal, we have computed LSPs of the other stars as well as the background itself, in case the signal was produced by artefacts from the electron noise in the detectors. We have not found any significant signal in any of these. In Figure 5, we present the LSP of the raw Epoch 4 g-band light curve for *GOTO 0650* (top panel), along with the LSP of the corresponding local background (bottom panel). Figure 5 shows a prominent peak in the periodogram of the raw flux at 6.7 mHz that is not seen in the periodogram of the local background. This rules out the 6.7 mHz signal being attributable to our reference stars, or a result of some instrumental/systematic effect, and instead suggests that the signal is intrinsic to *GOTO 0650*.

4 DISCUSSION

In Sec. 3, we have unambiguously found evidence of a periodic signal with a period of 148.5 ± 0.4 s in epoch 4 during the dip in between the main outburst and the beginning of the rebrightenings/echo-outburst of the newly discovered WZ-Sge-type CV *GOTO 0650*. Unfortunately, the weather conditions did not allow us to recover the signal from epoch 5, but the light curve from this night looks qualitatively similar. But, what is the origin of the 148.5 seconds signal observed in *GOTO 0650*? In this section, we will briefly explore the different physical mechanisms that can produce the observed signal.

This signal is present in g-band with its amplitude decreasing

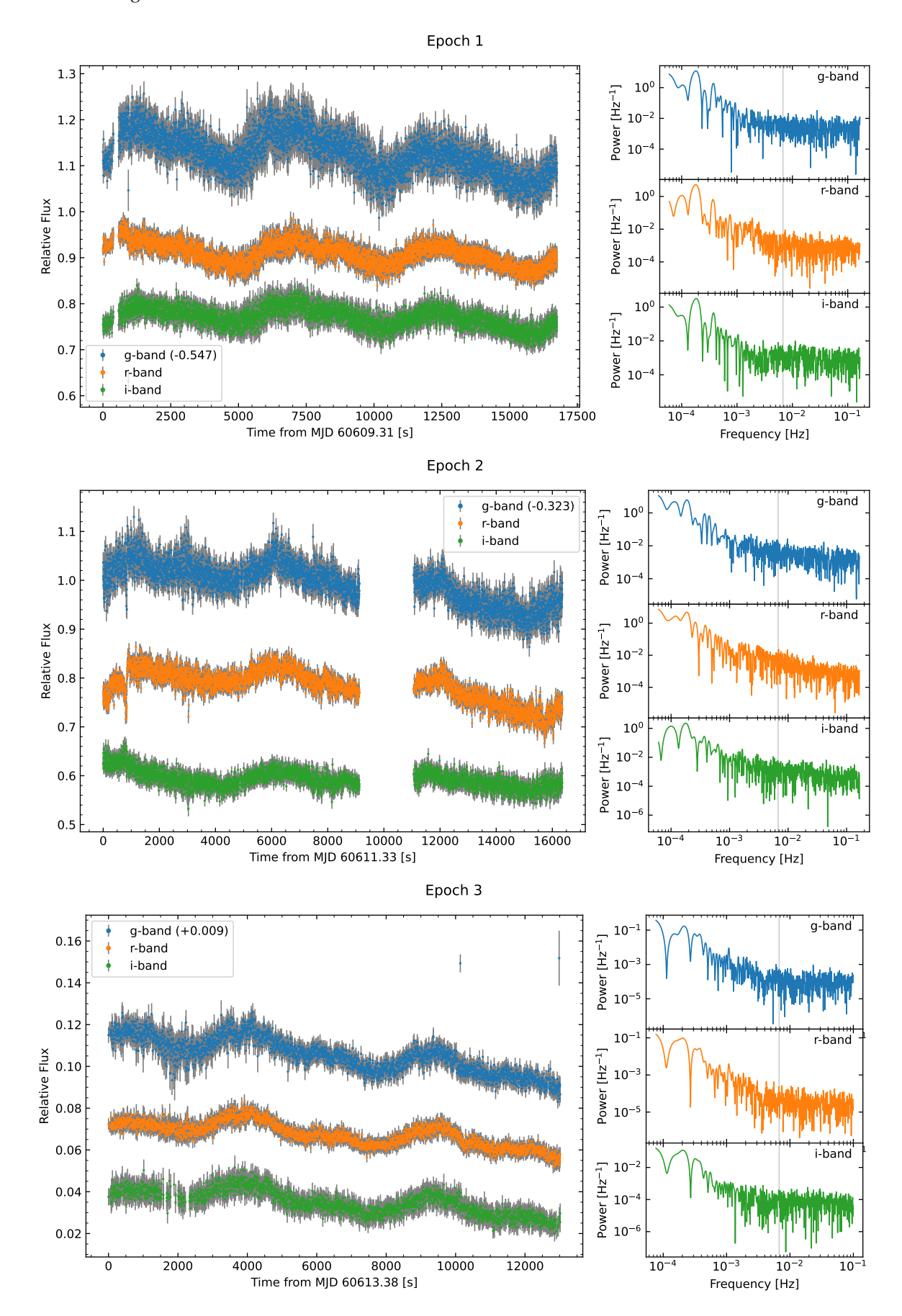


Figure 2. Relative light curves of all three cameras for epochs 1-3 (left panels), along with their respective periodograms (right panels). The vertical shaded region in the power spectra indicates the frequency at which we detect a statistically significant signal in epoch 4.

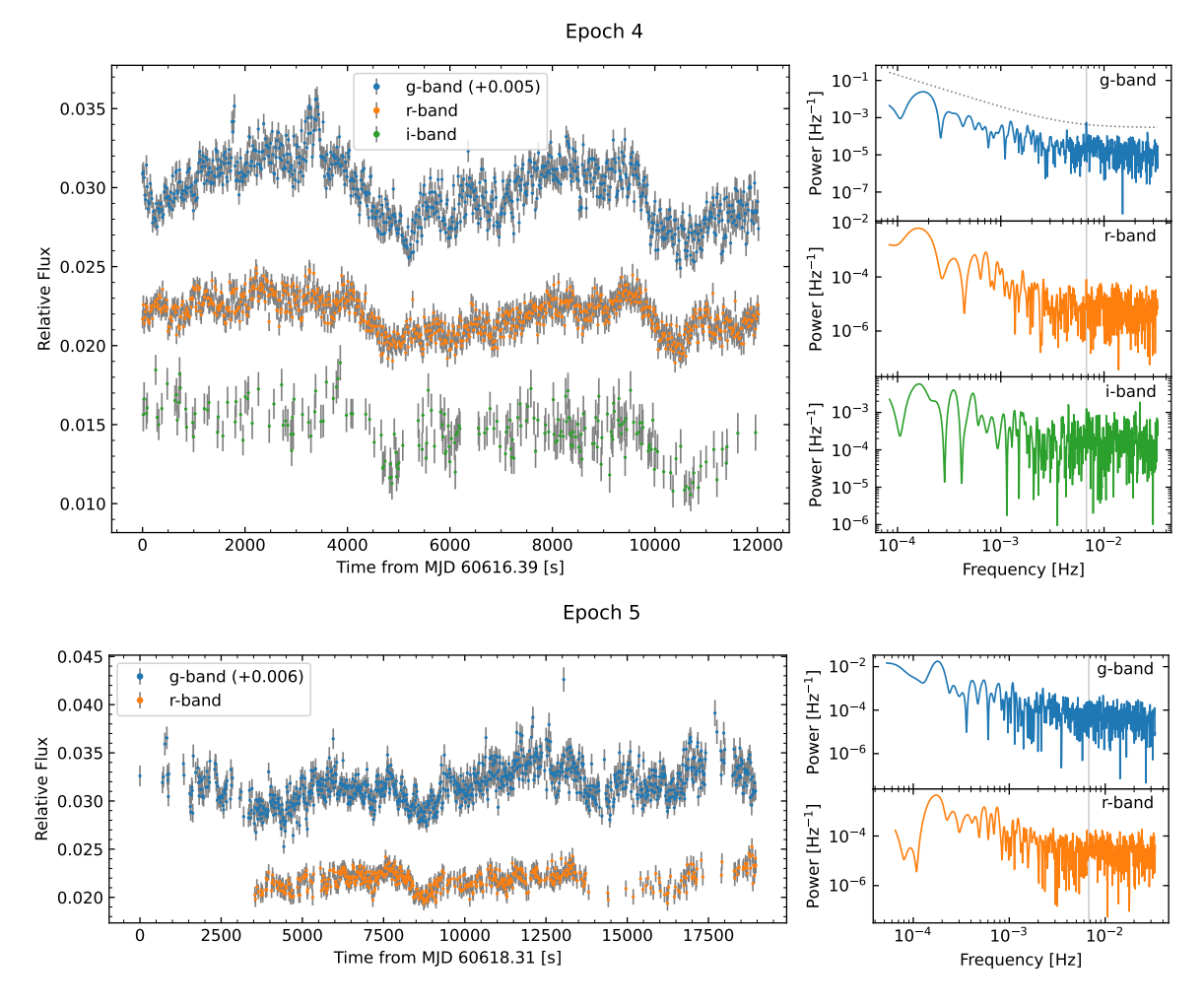


Figure 3. Same as Fig. 2 but for epochs 4 and 5. For the *g*-band periodogram in epoch 4, the 99.99 per cent confidence threshold is shown with a dotted line. The target was not detected in the *i* band during epoch 5, therefore, only *g* and *r* bands are shown.

toward longer wavelengths with a tentative detection in r-band. This suggests a blue spectral component generating the detected signal, similar to the one seen in IPs. In addition to this, the frequency of the observed signal is comparable with the dominant signal of a typical IP. This makes the $GOTO\ 0650$ a WZ Sge-type IP the most obvious interpretation, nonetheless we will consider other scenarios.

Dwarf nova oscillations (DNOs) have been proposed to explain some variable periodicity in outbursting CVs (e.g. Marsh & Horne 1998; Woudt & Warner 2002), these are vertically extended regions of the disc or blobs being irradiated by the hot WD and boundary layer, which produce a signal corresponding to their Keplerian orbit. These signals are typically of the order of 10 seconds and evolve to slightly lower frequencies as the outburst evolves (up to 40s). We do not detect any significant signal during the main outburst, therefore we discard this scenario. The accretion-induced heating from the outburst makes non-radial pulsations of the WD also unlikely since the temperature of the WD should be too hot to be in the instability strip (c.f. Clemens 1993; Toloza et al. 2016, but also see Szkody 2021), given its preoutburst temperature (Killestein et al. 2025). Finally, Veresvarska et al. (2024) proposed a precessing inner disc producing QPOs in a handful of CVs, however, these observed frequencies are typically one order of magnitude slower. Therefore we conclude that GOTO 0650 is likely a WZ Sge-IP, but, the stability of the signal would need to be tested once the system is back to quiescent levels.

Magnetism has been invoked to explain several properties of WZ Sge stars (see Sect. 1). WZ Sge itself is probably the most remarkable example of this class. This source exhibits fast optical, UV and Xray oscillations in quiescence (Robinson et al. 1978; Patterson 1980; Patterson et al. 1998; Skidmore et al. 1999) around 27.87s that have been associated with the spin period of the WD (Patterson et al. 1998). This signal is absent during outbursts owing to the combination of low magnetic field and/or low mass accretion rate from the donor, however, this interpretation has been challenged (c.f. Knigge et al. 2002), leaving the origin of this signal an enduring enigma. CC Scl and ASASSN-18fk are also proposed to harbour a slowly spinning WD (Woudt et al. 2012; Pavlenko et al. 2019; Paice et al. 2024). Another remarkable example of an intermediate polar exhibiting super-outbursts is V455 And (Araujo-Betancor et al. 2005; Bloemen et al. 2013), this system exhibits a spin period of 67.6 seconds with the dominant signal in the power spectrum being twice the spin period; however, it does not exhibit echo outbursts like GOTO 0650 and WZ Sge. The timescale of the signal observed in GOTO 0650 falls in-between that of CC Scl and V455 And, and the absence of the signal during outburst could be attributed to the combination of low magnetic field and/or mass transfer rate similar to what has been proposed for WZ Sge (Patterson et al. 1998). We then propose the observed signal as being produced by the spin period (or its first harmonic).

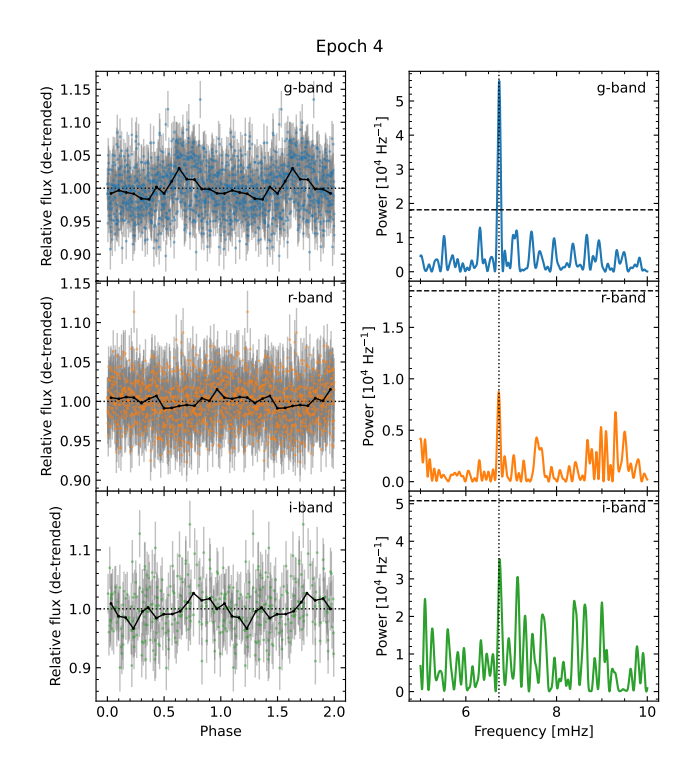


Figure 4. Left: Epoch 4 light curves folded on a period of 148.6 s (corresponding to 6.7 mHz), the black line represents the median values for the phase binned folded light curve, the zero phase is arbitrary but common across bands. Right: Epoch 4 LSPs. In the LSPs, the dotted vertical line corresponds to a frequency of 6.7 mHz and the horizontal line represents the 99.99 per cent confidence threshold.

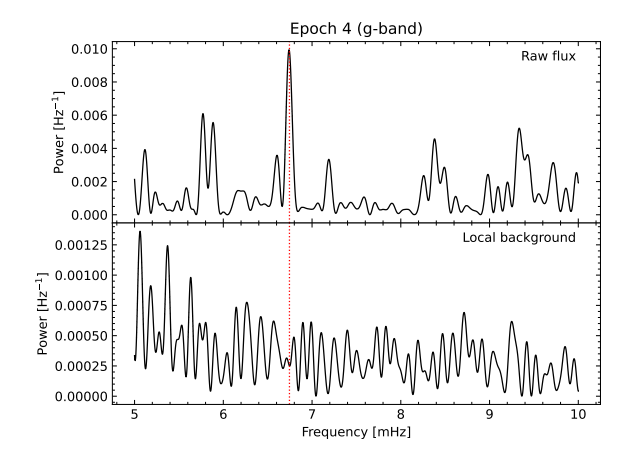


Figure 5. Top: LSP of *GOTO 0650*'s raw flux from Epoch 4 in the *g*-band; bottom: LSP of the corresponding local background.

The data from Epoch 4 was obtained 2-3 days after the decline from the main outburst; therefore, the disc and magnetic torques would have been far from equilibrium during this epoch, making any estimation of the magnetic field highly uncertain. However, we can set a lower limit on the magnetic field as the source's magnetospheric radius must be larger than the WD radius. To do this, we need to estimate the mass accretion rate; for a canonical mass transfer rate of $\dot{M}_{tr} \simeq 10^{-11} \ M_{\odot} \ yr^{-1}$ in WZ Sge stars (Knigge et al. 2011), typically expending $\gtrsim 30$ years in quiescence between outbursts, and

with an outburst duration of $\simeq 30$ d, we estimate the average mass accretion rate during the outburst to be $<\dot{M}_{acc}>\simeq 7\times 10^{-9}~{\rm M}_{\odot}~{\rm yr}^{-1}$ in a conservative mass transfer scenario. Alternatively we can obtain the peak mass accretion rate via the peak absolute magnitude MV vs orbital period (P_{orb}) and its relation with \dot{M}_{acc} (e.g. Warner 1987; Patterson 2011). For a source close to the period minimum (as GOTO 0650 is), we find the absolute magnitude at (super outburst) peak to be $M_V \simeq 5$, consistent with the value derived by Killestein et al. (2025). In turn, this value give us an estimation of the mass accretion rate of $\dot{M}_{acc} \simeq 2 \times 10^{-8} \,\mathrm{M}_{\odot} \,\mathrm{yr}^{-1}$ (e.g. Warner 1987). We can therefore assume $\dot{M}_{acc} \sim 10^{-8} \ M_{\odot} \ yr^{-1}$ a reasonable mass accretion rate during the main outburst of GOTO 0650. During Epoch 4 the source was 2 orders of magnitude fainter, therefore, assuming the bulk observed luminosity during this epoch being dominated by the accretion disc and given that this scales with the mass accretion rate $(L_{acc} \propto \dot{M}_{acc})$, we can adopt $\dot{M}_{acc} \sim 10^{-10}~M_{\odot}~yr^{-1}$ during epoch 4 as a reasonable approximate reference value for our calculations (acknowledging that it excludes corrections or additional spectral components; e.g., the hot spot). If the magnetosphere of the white dwarf truncates the disc at the co-rotation radius, i.e. $r_M = \xi r_A = r_{CO}$ (with $\xi \simeq 0.5$ e.g. Ghosh & Lamb 1979; Long et al. 2005), we can set a lower limit of the magnetic field, B, at which $r_M = R_{WD}$. For a typical 0.8 M_☉ WD in a CV (Zorotovic et al. 2011; Pala et al. 2017). this would give us a lower limit of B $\sim 2 \times 10^4$ G. This argument cannot be used for Epoch 3, since the disc is experiencing a rapid change which will keep it even further from a stationary configuration. The same is not true for Epoch 2, thus allowing us to set an upper limit in the magnetic field strength. Assuming the disc "pushed" magnetosphere to the surface of the WD during the outburst, we can constrain the magnetic field to be $B \leq 4 \times 10^4 G$.

In the hypothetical case of the disc and magnetic torques being in equilibrium during Epoch 4, we could estimate the magnetic field of the system, for $P_{\omega}=1$ and $2\times P_{spin}$ this would correspond to a magnetic field of 5×10^4 G and 10^5 G respectively. The latter of these values would require a $\dot{M}_{acc}\simeq 10^{-7}~\rm M_{\odot}~\rm yr^{-1}$ to push the magnetosphere down to the WD surface, this scenario not only goes against our constraints from above but it would make the system enter a super-Eddington wind regime (c.f. Ma et al. 2013). We therefore suggest that P_{ω} may be the fundamental frequency of the spin period, and the WD's magnetic would be of the order of $B\sim 10^4~G$. However, quiescent observations are required to test this hypothesis. If confirmed, GOTO~0650 would not only be another example of how magnetic fields can be dynamically important in highly evolved CVs but also would bridge the gap between intermediate- and fast-rotating AWDs.

ACKNOWLEDGEMENTS

We are grateful to the referee for their helpful feedback. We are grateful to many amateur astronomers for making their data publicly available in *AAVSO*. NCS and DLC acknowledges support from the Science and Technology Facilities Council (STFC) grant ST/X001121/1. ZAI, FV and DA acknowledges support STFC grants ST/V001000/1 and ST/X508767/1. IP acknowledges support from a Royal Society University Research Fellowship (URF\R1\231496). AC acknowledges support from the Royal Society Newton International Fellowship grant NF170803. Based upon observations carried out at the Observatorio Astronómico Nacional on the Sierra San Pedro Mártir (OAN-SPM), Baja California, México. We thank I. Zavala for maintaining the data acquisition software of OPTICAM.

Kimura M., et al., 2018, PASJ, 70, 47

Killestein T. L., et al., 2025, arXiv e-prints, p. arXiv:2501.11524

Kimura M., Osaki Y., Kato T., Mineshige S., 2020, PASJ,

AFFILIATIONS

- ¹Department of Physics, University of Warwick, Gibbet Hill Road, Coventry, CV4 7AL, UK
- ²Department of Physics & Astronomy. University of Southampton, Southampton SO17 1BJ, UK.
- ³South African Astronomical Observatory, PO Box 9, Observatory, 7935, Cape Town, South Africa
- ⁴Department of Astronomy, University of Cape Town, Private Bag X3, Rondebosch 7701, South Africa
- ⁵Instituto de Astronomía, Universidad Nacional Autónoma de México, Carretera Tijuana-Ensenada Km. 107, Ensenada, B.C. 22860, México
- ⁶SUPA School of Physics and Astronomy, University of St Andrews, North Haugh, St Andrews KY16 9SS, Scotland, UK
- ⁷Centre for Extragalactic Astronomy, Department of Physics, Durham University, South Road, Durham, DH1 3LE
- ¹⁰NAF Osservatorio Astronomico di Capodimonte, Salita Moiariello 16, I-80131 Naples, Italy
- ⁸Advanced Research Center for Space Science and Technology, College of Science and Engineering, Kanazawa University, Kakuma, Kanazawa, Ishikawa 920-1192, Japan

DATA AVAILABILITY

The data underlying this article is publicly available in AAVSO https://www.aavso.org and ZTF https://www.ztf. caltech.edu/ztf-public-releases.html. The remaining data will be shared on reasonable request to the corresponding author.

REFERENCES

```
Araujo-Betancor S., et al., 2005, A&A, 430, 629
Bellm E. C., et al., 2019a, PASP, 131, 018002
Bellm E. C., et al., 2019b, PASP, 131, 068003
Belloni T., Psaltis D., van der Klis M., 2002, ApJ, 572, 392
Bhattacharya S., Bhattacharyya S., 2024, The Astronomer's Telegram, 16866,
Bloemen S., Steeghs D., De Smedt K., Vos J., Gänsicke B. T., Marsh T. R.,
    Rodriguez-Gil P., 2013, MNRAS, 429, 3433
                  et
                          al.,
                                  2024,
                                            astropy/photutils:
           L..
    doi:10.5281/zenodo.12585239,
                                          https://doi.org/10.5281/
    zenodo.12585239
Campana S., Stella L., Mereghetti S., de Martino D., 2018, A&A, 610, A46
Castro Segura N., et al., 2021, MNRAS, 501, 1951
Castro A., et al., 2019, Rev. Mex. Astron. Astrofis., 55, 363
Castro A., et al., 2024, New Astron., 112, 102262
Clemens J. C., 1993, Baltic Astronomy, 2, 407
Dyer M. J., et al., 2024, in Marshall H. K., Spyromilio J., Usuda T., eds,
    Society of Photo-Optical Instrumentation Engineers (SPIE) Conference
    Series Vol. 13094, Ground-based and Airborne Telescopes X. p. 130941X
    (arXiv:2407.17176), doi:10.1117/12.3018305
Eracleous M., Horne K., 1996, ApJ, 471, 427
Georganti M., Knigge C., Castro Segura N., Long K. S., 2022, MNRAS, 511,
    5385
```

Ghosh P., Lamb F. K., 1979, ApJ, 234, 296

Kato T., 2015, PASJ, 67, 108

Hameury J. M., 2020, Advances in Space Research, 66, 1004

Killestein T., et al., 2024a, The Astronomer's Telegram, 16842, 1 Killestein T., et al., 2024b, The Astronomer's Telegram, 16858, 1

Ivezić Ž., Connolly A. J., VanderPlas J. T., Gray A., 2014, Statistics, Data Mining, and Machine Learning in Astronomy: A Practical Python Guide for the Analysis of Survey Data, doi:10.1515/9781400848911.

```
Knigge C., Hynes R. I., Steeghs D., Long K. S., Araujo-Betancor S., Marsh
    T. R., 2002, ApJ, 580, L151
Knigge C., Baraffe I., Patterson J., 2011, ApJS, 194, 28
Lasota J.-P., 2016, Black Hole Accretion Discs. p. 1, doi:10.1007/978-3-662-
    52859-4 1
Littlefield C., Scaringi S., Garnavich P., Szkody P., Kennedy M. R., Iłkiewicz
    K., Mason P. A., 2021, AJ, 162, 49
Lomb N. R., 1976, Ap&SS, 39, 447
Long M., Romanova M. M., Lovelace R. V. E., 2005, ApJ, 634, 1214
Ma X., Chen X., Chen H.-l., Denissenkov P. A., Han Z., 2013, ApJ, 778, L32
Marsh T. R., Horne K., 1998, MNRAS, 299, 921
McCully C., et al., 2018, astropy/astroscrappy: v1.0.5 Zenodo Release,
    doi:10.5281/zenodo.1482019
Naylor T., 1998, MNRAS, 296, 339
Paice J. A., et al., 2024, MNRAS, 531, L82
Pala A. F., et al., 2017, MNRAS, 466, 2855
Patterson J., 1980, ApJ, 241, 235
Patterson J., 2011, MNRAS, 411, 2695
Patterson J., Richman H., Kemp J., Mukai K., 1998, PASP, 110, 403
Patterson J., et al., 2005, PASP, 117, 1204
Pavlenko E., et al., 2019, Contributions of the Astronomical Observatory
    Skalnate Pleso, 49, 204
Robinson E. L., Nather R. E., Patterson J., 1978, ApJ, 219, 168
Scargle J. D., 1982, ApJ, 263, 835
Skidmore W., Welsh W. F., Wood J. H., Catalán M. S., Horne K., 1999,
    MNRAS, 310, 750
Smak J., 1993, Acta Astron., 43, 101
Smak J., 2009, Acta Astron., 59, 121
Southworth J., Gänsicke B. T., Marsh T. R., de Martino D., Hakala P., Littlefair
    S., Rodríguez-Gil P., Szkody P., 2006, MNRAS, 373, 687
Steeghs D., et al., 2022, MNRAS, 511, 2405
Szkody P., 2021, Frontiers in Astronomy and Space Sciences, 8, 184
Tampo Y., 2024, GOTO065054.49+593624.51: type-E rebrightening WZ
    Sge star?, http://ooruri.kusastro.kyoto-u.ac.jp/mailman3/
    hvperkitty/list/vsnet-alert@ooruri.kusastro.kvoto-u.
    ac.jp/thread/TWMZC3AKMJHBRPUBNRLYHGTKDCJKITDQ/
Toloza O., et al., 2016, MNRAS, 459, 3929
VanderPlas J. T., 2018a, ApJS, 236, 16
VanderPlas J. T., 2018b, ApJS, 236, 16
Vaughan S., 2005, A&A, 431, 391
Vaughan S., Edelson R., Warwick R. S., Uttley P., 2003, MNRAS, 345, 1271
Veresvarska M., et al., 2024, MNRAS, 534, 3087
Warner B., 1987, MNRAS, 227, 23
Warner B., 1995, Cataclysmic variable stars. Vol. 28
Woudt P. A., Warner B., 2002, MNRAS, 333, 411
Woudt P. A., et al., 2012, MNRAS, 427, 1004
Zorotovic M., Schreiber M. R., Gänsicke B. T., 2011, A&A, 536, A42
van Dokkum P. G., 2001, PASP, 113, 1420
This paper has been typeset from a TEX/LATEX file prepared by the author.
```